

Reversible and irreversible effects after oxygen exposure in thick ($>1 \mu\text{m}$) silicon films deposited by VHF-PECVD on glass substrates investigated by dual beam photoconductivity¹

Gökhan Yılmaz, Hamza Cansever, H. Muzaffer Sagban, Mehmet Günes, Vladimir Smirnov, Friedhelm Finger, and Rudi Brüggemann

Abstract: Metastability and instability effects due to oxygen exposure in thick intrinsic hydrogenated microcrystalline silicon films deposited by very high frequency plasma enhanced chemical vapour deposition on smooth glass substrates were investigated using temperature-dependent dark conductivity, steady state photoconductivity, and sub-bandgap absorption measurements obtained using the dual beam photoconductivity (DBP) method. No significant changes in dark conductivity and photoconductivity were detected even after long-term air exposure of samples in room ambient as well as after oxygen exposure when samples were characterized in oxygen ambient. However, characterization of the oxygen-exposed state in high vacuum caused an increase in dark conductivity and photoconductivity as well as a significant decrease in the sub-bandgap absorption coefficient spectra in the low energy region in samples with $I_C^{\text{RS}} > 0.40$. These changes are partially irreversible for samples $I_C^{\text{RS}} > 0.80$ and mostly reversible for compact materials with significant amorphous fraction. No detectable metastable changes occurred in microcrystalline silicon samples with $I_C^{\text{RS}} < 0.40$ as well as in pure amorphous silicon.

PACS Nos.: 73.61.Jc, 73.63.Bd, 73.50.Pz, 72.80.Ng.

Résumé : Nous utilisons la conductivité en obscurité, la photoconductivité stationnaire et des mesures d'absorption sous la bande interdite obtenues de la méthode de photoconductivité à deux faisceaux (DBP), afin d'étudier les effets stables et métastables de l'exposition à l'oxygène de films de silicium microcristallins hydrogénés épais déposés par plasma à haute fréquence augmenté d'un dépôt de vapeur chimique sur un substrat de verre lisse. Nous ne détectons aucun changement de la conductivité en obscurité ni de la photoconductivité, même après une longue exposition à l'air à température ambiante, aussi bien qu'après exposition à l'oxygène où les échantillons sont examinés dans une atmosphère d'oxygène. Cependant, étudier sous vide les échantillons exposés à l'oxygène donne une augmentation de la conductivité en obscurité, aussi bien que de la photoconductivité, en même temps qu'une diminution significative de l'absorption sous la bande interdite dans les échantillons avec $I_C^{\text{RS}} > 0.40$. Ces changements sont partiellement réversibles pour les échantillons avec $I_C^{\text{RS}} > 0.80$ et majoritairement réversibles pour les matériaux compacts avec une fraction amorphe importante. Nous ne détectons aucun changement métastable dans les échantillons de silicium microcristallin avec $I_C^{\text{RS}} < 0.40$ ni dans le silicium complètement amorphe. [Traduit par la Rédaction]

1. Introduction

Single junction and multijunction thin-film silicon solar cells are generally deposited on rough light-scattering substrates with absorber layers of undoped hydrogenated amorphous and microcrystalline silicon ($\mu\text{c-Si:H}$) layers with thickness about $1 \mu\text{m}$ or higher [1, 2]. Long-term stability of such solar cell structures is mainly determined by the properties of absorber layers as well as interfaces and contacts. Amorphous silicon absorber layers strongly suffer from the metastability called the Staebler–Wronski effect [3]. Solar cells having $\mu\text{c-Si:H}$ absorber layers with significant crystalline volume fraction were demonstrated to be immune to the Staebler–Wronski effect [1]. However, such $\mu\text{c-Si:H}$ layers were reported to exhibit different types of instability and metastability phenomena under air or oxygen exposure [4]. The former is due to irreversible formation of Si–O bonds on the grain boundaries as identified by infrared spectroscopy. The latter is the

reversible adsorption of oxygen, which strongly decreases electrical conductivity by several orders of magnitude and increase the electron spin resonance spin density [4]. Two decades later, it was shown that two different metastable changes in dark conductivity exist in microcrystalline silicon, where σ_{Dark} generally decreases in highly crystalline materials (called type I) and it increases in more compact materials (called type II) with significant amorphous fraction as samples are exposed to air or oxygen [5]. Corresponding electron spin resonance investigation carried out using powder samples indicated irreversible changes in spin density in highly crystalline materials with $I_C^{\text{RS}} > 0.70$ after oxygen treatment at 80°C . However, no significant change in electron spin resonance spins was detected in compact samples with $I_C^{\text{RS}} < 0.50$ [5, 6]. Investigation of metastability and instability effects using photoconductivity methods like steady-state photoconductivity, steady-state photocarrier grating method, transient photoconductivity,

Received 25 October 2013. Accepted 22 November 2013.

G. Yılmaz, H. Cansever, H.M. Sagban, and M. Günes. Mugla Sitki Koçman University, Faculty of Sciences, Physics Department, Köekli Yerleskesi, 48000 Muğla, Turkey.

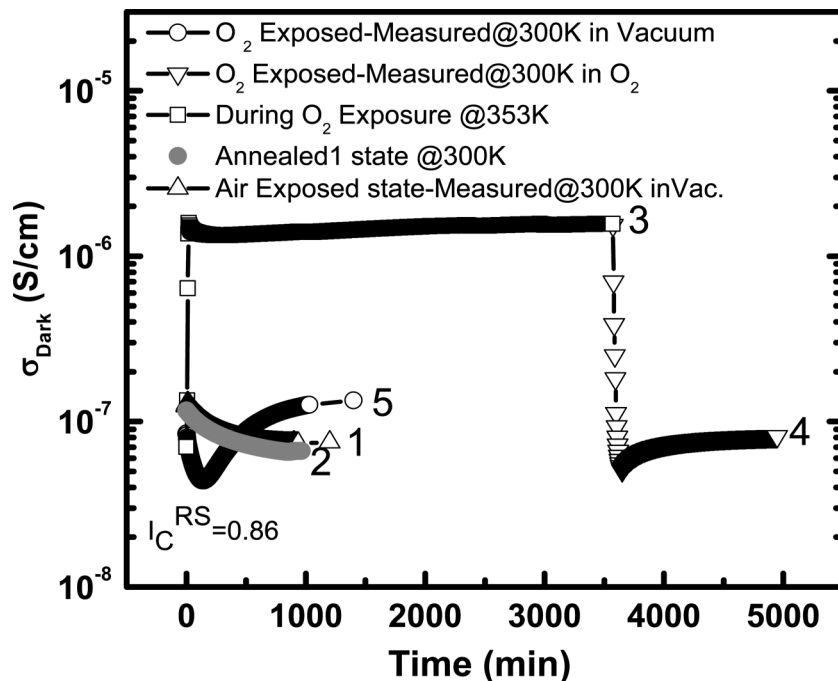
V. Smirnov and F. Finger. Forschungszentrum Jülich, IEK-5 Photovoltaik 52425 Jülich, Germany.

R. Brüggemann. Institut für Physik, Carl von Ossietzky Universität Oldenburg, 26111 Oldenburg, Germany.

Corresponding author: Mehmet Günes (e-mail: mehmet.gunes@mu.edu.tr).

¹This paper was presented at the 25th International Conference on Amorphous and Nanocrystalline Semiconductors (ICANS25).

Fig. 1. Time dependence of the dark conductivity for 1.268 μm thick microcrystalline silicon with $I_C^{\text{RS}} = 0.86$ for different experimental condition: (1) air exposed sample measured in vacuum; (2) annealed1 state measured in vacuum (gray); (3) oxygen exposed measured at 353 K in O_2 ambient; (4) oxygen exposed measured at 300 K in O_2 ambient; and (5) oxygen exposed measured at 300 K in vacuum, for which time scale starts from zero.



and sub-bandgap absorption spectroscopy techniques, such as photothermal deflection spectroscopy, constant photocurrent method, and dual beam photoconductivity (DBP), require samples deposited on smooth glass substrates. Adhesion of silicon layers on smooth glass substrates with thickness larger than $1 \mu\text{m}$ is a major problem due to poor adhesion as a result of internal stress in the films. For this reason, most of our earlier results on the metastability due to atmospheric exposures have only concerned thin silicon layers of a typical thickness less than $0.3 \mu\text{m}$ [5–10]. As it is generally found that $\mu\text{c-Si:H}$ has a considerable change in its structural properties as a function of thickness, it is of interest to what extent properties of such thin films represent bulk properties of material of more than $1 \mu\text{m}$ as used in solar cells. To improve film adhesion and allow deposition of thick microcrystalline silicon films, rough glass substrates have been used to investigate the metastability phenomena in the bulk materials [10]. However, most optical methods cannot be applied reliably in such films due to the strong light scattering of the rough substrates.

In the present study, a new approach has been used to deposit microcrystalline silicon films thicker than $1 \mu\text{m}$ on smooth glass substrates by using very thin a-SiO_x (10–30 nm) interlayers deposited on the substrate before silicon deposition. The a-SiO_x layers improve film adhesion considerably. On the other hand, the SiO_x films are highly transparent in the optical wavelength range of interest so they have negligible effect on the data in our experimental methods, in particular steady-state photoconductivity and defect spectroscopy with the DBP method. Sub-bandgap absorption coefficient spectra obtained using DBP are a powerful tool to investigate the changes in the occupation of defect states in the light-soaked and annealed states of a-Si:H films [11] and are also very sensitive to study bulk defects in $\mu\text{c-Si:H}$ films [12]. Preliminary results obtained with the DBP method indicated that reversible and irreversible changes created by water and (or) oxygen exposure can be detected by the changes in the sub-bandgap absorption coefficient spectrum [13].

Applying the DBP method together with temperature-dependent dark conductivity and steady-state photoconductivity measurements we studied reversible and irreversible effects due to oxygen exposure in the bulk of thick microcrystalline silicon films with varying microstructure grown on SiO_x adhesion layers on smooth glass substrates.

2. Experimental details

Thin (10 – 30 nm) a-SiO_x layers were deposited by e-beam assisted evaporation on the smooth glass substrates. Undoped intrinsic silicon films thicker than $1 \mu\text{m}$ were deposited using very high frequency – plasma enhance chemical vapor deposition (VHF-PECVD) under varying silane concentrations at substrate temperature 200°C on these SiO_x covered smooth glass substrates. Crystalline volume fraction, I_C^{RS} , of the samples was determined from Raman measurements. Material with crystalline volume fraction between 0% (amorphous) and 86% (highly crystalline) were deposited and investigated. It is assumed that material with high crystallinity (>60%) has a pronounced porosity and is possibly more affected by atmospheric gas in-diffusion, while material with lower crystallinity is likely more compact [5, 6]. Silver coplanar electrodes were evaporated on the samples with 0.5 cm length and 0.5 mm separation. A collimated He–Ne laser light source was used to measure steady-state photoconductivity, σ_{photo} , under Ohmic DC bias. The intensity of light was reduced using neutral density filters. A standard measurement procedure [14] based on real-time monitoring of dark conductivity, σ_{Dark} , was used to obtain steady-state level of σ_{Dark} in the annealed and oxygen exposed states before applying the steady-state methods. The DBP method with different DC bias light intensities and optical transmission simultaneously measured from the back of the sample were used to calculate absolute absorption coefficient spectra of the samples by using Ritter–Weiser optical equations [15]. Homogeneously absorbed red light obtained using a long pass filter with $\lambda > 650 \text{ nm}$ was used as DC bias light. Samples were

exposed to laboratory atmosphere in dark for more than a year and to a controlled high-purity oxygen gas atmosphere in a cryostat for several days. Temperature of the samples was increased to 80 °C during oxygen treatment. Annealing took place at 430 K in vacuum and in dark. All probe measurements were performed at 300 K in exposing gas ambient as well as in high vacuum of $2\text{--}3 \times 10^{-6}$ mbar as σ_{Dark} remained constant, where the percent change in σ_{Dark} , $\Delta\sigma_{\text{Dark}}$, was within less than 10% during the several hours of measurements.

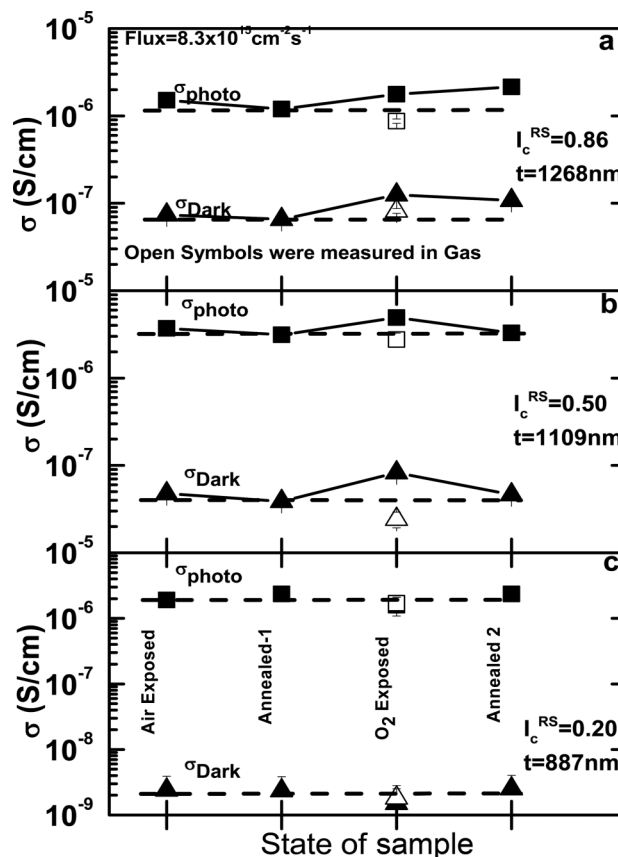
3. Results and discussion

Time dependence of dark conductivity for 1.26 μm thick microcrystalline silicon with $I_{\text{C}}^{\text{RS}} = 0.86$ is shown in Fig. 1 during oxygen treatment and vacuum development after air and oxygen exposure. Long term air exposed sample in vacuum requires almost 1000 min to get stabilized dark conductivity. After performing the probe measurements, sample was annealed at 430 K and cooled to 300 K. There was no significant change in σ_{Dark} between air exposed (curve 1) and annealed states (curve 2). As high purity oxygen is purged in the cryostat as sample heated to 80 °C, σ_{Dark} increased drastically due to both temperature and oxygen and very slowly reached a constant level in O_2 ambient. At the end of 60 h exposure, sample was cooled to 300 K in O_2 ambient and σ_{Dark} was recorded until a constant level obtained (curve 4). σ_{Dark} after this treatment was very similar to the value after the first annealing within 10% as seen in Fig. 1. However, σ_{Dark} of oxygen exposed sample in vacuum decreased initially during the establishment of vacuum, then increased slowly and reached a constant level at the end of 16 h pumping. Vacuum treatment after oxygen exposure results in an irreversible increase in σ_{Dark} within a factor of two, which is much less than seen in thin samples under similar conditions [8, 16].

Steady state photoconductivity measurements of the sample were carried out as σ_{Dark} was constant in the annealed and exposed states. A summary of changes in σ_{Dark} and σ_{photo} is presented in Fig. 2a for the sample with $I_{\text{C}}^{\text{RS}} = 0.86$. Both results showed an irreversible increase within a factor of two after oxygen exposure and following annealing. Similar measurements were also performed in other thick microcrystalline silicon films. In Figs. 2b and 2c, the results are shown for the presumably more compact films with $I_{\text{C}}^{\text{RS}} = 0.50$ and 0.20, respectively. Similar to the results for the highly crystalline sample there is no change in σ_{Dark} and σ_{photo} between the air exposed and the annealed1 states of both samples. The sample with $I_{\text{C}}^{\text{RS}} = 0.50$ showed a metastable increase only after vacuum treatment of the oxygen exposed state. The changes in σ_{Dark} and σ_{photo} were completely reversible after annealing. For the sample with even lower crystallinity ($I_{\text{C}}^{\text{RS}} = 0.20$) the changes in conductivities were very small as shown in Fig. 2c. It can be inferred from these results that thick $\mu\text{c-Si:H}$ films with low crystallinity and presumable compact structure are not affected seriously from oxygen exposure, different from the findings on thin (<300 nm) sample in earlier studies [5, 7–10], while thick highly crystalline porous samples still show irreversible changes of their properties upon exposure to oxygen. The results are consistent with previous reports on the thickness dependence of changes due to atmospheric exposures, where sensitivity to gas exposure decreased with increasing thickness of the samples [8].

To correlate the conductivity changes between annealed and oxygen exposed states, DBP measurements under different DC bias light intensity were carried out in thick $\mu\text{c-Si:H}$ films. In Fig. 3, DBP yield spectra of $\mu\text{c-Si:H}$ film with $I_{\text{C}}^{\text{RS}} = 0.86$ are presented for four different DC bias light intensity in the annealed1 state together with optical transmission spectra of the sample. DBP yield in the sub-bandgap energy region increase with increased DC bias light intensity due to increased density of occupied defect states in the bandgap as quasi Fermi levels move closer

Fig. 2. Summary of σ_{Dark} and σ_{photo} measured in the air exposed, oxygen exposed, and annealed states carried out before and after oxygen treatment for $\mu\text{c-Si:H}$ samples with (a) $I_{\text{C}}^{\text{RS}} = 0.86$, (b) $I_{\text{C}}^{\text{RS}} = 0.50$, and (c) $I_{\text{C}}^{\text{RS}} = 0.20$.



to the band edges. We have used the DBP yield spectrum measured with the lowest DC bias light (curve 1 in Fig. 3) to compare the reversible and irreversible changes in the absolute absorption coefficient, $\alpha(h\nu)$, spectrum between annealed and oxygen exposed states among the samples, which corresponds to the occupied defect distribution below the Fermi level as close as possible to that in the dark condition. The $\alpha(h\nu)$ spectrum was calculated using the DBP yield and optical transmission spectra shown in Fig. 3 together with the Ritter–Weiser optical equations [15].

In Fig. 4a, the $\alpha(h\nu)$ spectra of $\mu\text{c-Si:H}$ film with $I_{\text{C}}^{\text{RS}} = 0.86$ are presented in the annealed states as well as oxygen exposed state measured in high vacuum. The remaining interference fringes in the $\alpha(h\nu)$ spectra are the indication of inhomogeneous absorption of light in such thick $\mu\text{c-Si:H}$ films. The $\alpha(h\nu)$ spectra for air exposed and oxygen exposed state measured in O_2 ambient were almost identical to that of annealed1 state (data not shown for clarity). However, the $\alpha(h\nu)$ spectrum of oxygen exposed state measured in high vacuum showed a factor of five decrease in the low energy region of spectrum, indicating a decrease in the density of electron occupied defect states below the Fermi level. The change in the $\alpha(h\nu)$ spectrum was partially reversible after the second annealing. However, it was significantly lower than that measured before the oxygen treatment. Irreversible decrease in the $\alpha(h\nu)$ spectrum corresponds to a decrease in the density of electron occupied defect states in the oxygen exposed state, which should eventually increase the majority carrier $\mu\tau$ -products and steady state photoconductivity. This is to some extent confirmed by the data shown in Fig. 2a.

Fig. 3. Dual beam photoconductivity yield spectra measured under different DC bias intensities (from (1) the lowest to (4) the highest) for the 1.268 μm thick $\mu\text{c-Si:H}$ with $I_C^{\text{RS}} = 0.86$ in the annealed state. To indicate the relative changes in sub-bandgap energies, the spectra were normalized in the higher energy region. In the inset, optical transmission spectrum of the same sample is shown.

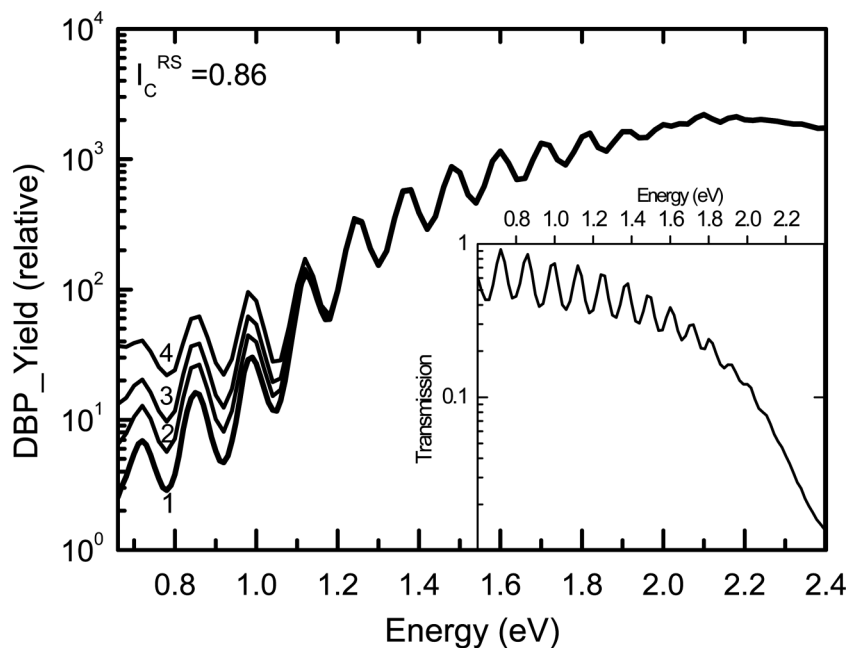
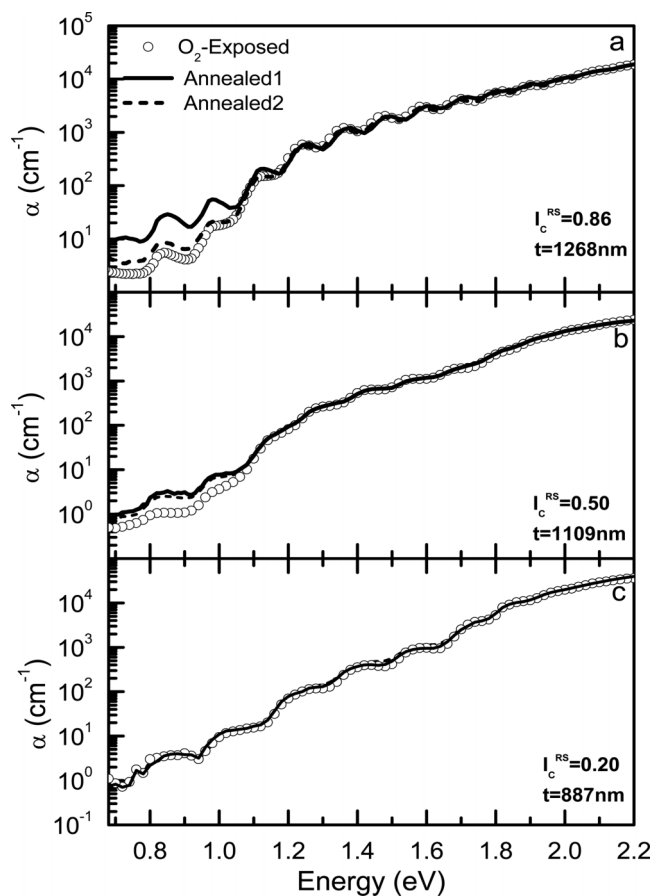


Fig. 4. Sub-bandgap absorption coefficient spectra calculated using the lowest DC bias DBP yield and optical transmission spectra of $\mu\text{c-Si:H}$ films (a) $I_C^{\text{RS}} = 0.86$, (b) $I_C^{\text{RS}} = 0.50$, and (c) $I_C^{\text{RS}} = 0.20$, in the oxygen exposed state and annealed states.

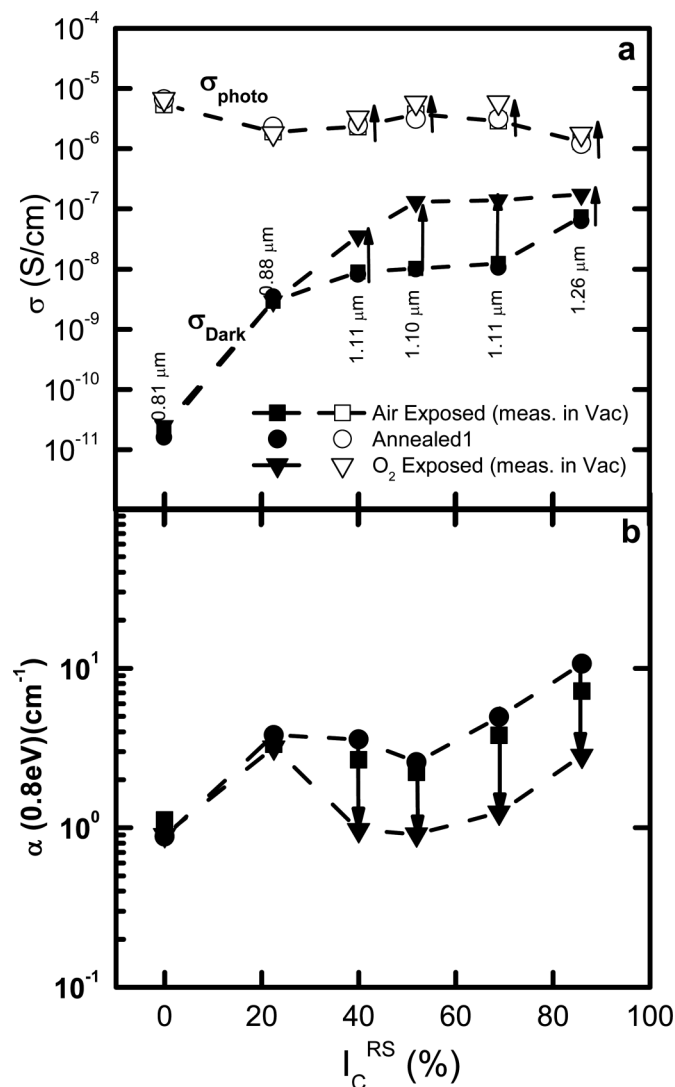


The effect of oxygen on the $\alpha(h\nu)$ spectrum for the low crystallinity compact materials are shown in Figs. 4b and 4c for samples with $I_C^{\text{RS}} = 0.50$ and 0.20 , respectively. For the compact sample with $I_C^{\text{RS}} = 0.50$, the $\alpha(h\nu)$ spectrum decreased by a factor of three after oxygen exposure. The change in the $\alpha(h\nu)$ is less than that of highly crystalline porous sample and totally reversible as shown in Fig. 4b. The results of σ_{Dark} and σ_{photo} presented in Fig. 2 also support the metastable changes for this compact sample. For the low crystalline sample with $I_C^{\text{RS}} = 0.20$, there was no detectable change in the $\alpha(h\nu)$ spectra after oxygen treatment as consistent with the results of σ_{Dark} and σ_{photo} presented in Fig. 2c.

A summary of oxygen-induced changes observed in thick $\mu\text{c-Si:H}$ films is shown in Fig. 5 as a function of crystalline volume fraction. It is a general trend that thick ($1 \mu\text{m}$) silicon samples, different from the thin ($<300 \text{ nm}$) films studied earlier [5, 7–10], were not affected by the long-term air exposure when the samples were kept in the laboratory atmosphere. Even after oxygen exposure when samples were characterized in oxygen ambient, very little change was detected. Surprisingly the effect of oxygen exposure can only be observed as samples were characterized in high vacuum. For samples with $I_C^{\text{RS}} > 0.40$, σ_{Dark} and σ_{photo} increased within factor of 2–10 in the oxygen exposed state. For lower crystalline and amorphous silicon samples no change was detected. The results observed in a-Si:H film are also consistent with the earlier reports that oxygen does not react as easily with the surface of a-Si:H because of the presence of hydrogen passivating the defects on the surface (see the review by Fritzsche [18]). Time-dependent dark conductivity recorded during oxygen exposure and vacuum development were found to be reproducible for other thick silicon films as shown in Fig. 1, where a small dip in dark conductivity existed at the initial stage of vacuum development for samples with $I_C^{\text{RS}} > 0.70$.

The sub-bandgap absorption coefficient $\alpha(h\nu)$ at 0.8 eV shown in Fig. 5b decreased within a factor of 2–5 for samples with $I_C^{\text{RS}} > 0.40$ in the oxygen exposed state. These changes are mostly permanent for the highly crystalline porous sample with $I_C^{\text{RS}} = 0.86$. Reversible changes dominate in the compact samples. The revers-

Fig. 5. Summary of the results measured in the air exposed, annealed, and oxygen exposed states in high vacuum (a) σ_{Dark} and σ_{photo} , (b) absorption coefficient $\alpha(h\nu)$ at 0.8 eV, as a function of crystalline volume fraction I_C^{RS} for thick $\mu\text{c-Si:H}$ films.



ible and irreversible changes caused by the oxygen treatment in $\mu\text{c-Si:H}$ films thicker than 1 μm indicate that oxygen creates irreversible instability effects in highly crystalline porous films. The reasons are most likely chemical bonding of oxygen on the surface of crystalline grains [4], which cause a surface charge and resulting band bending and passivate the defects. Reversible metastable changes due to adsorption of oxygen are found in the compact samples with $I_C^{\text{RS}} < 0.70$ [4–8]. Because these changes are rather small as compared to those observed in thin samples reported in previous studies for both class of materials [8], it can be inferred that oxygen cannot penetrate through the bulk of the film and the

observed changes occur mainly at the top surface region of the samples even for highly crystalline material.

4. Summary and conclusion

We have used thin e-beam evaporated a-SiO_x interlayers to improve the adhesion of $\mu\text{c-Si:H}$ films thicker than 1 μm grown by VHF-PECVD on smooth glass substrates and investigated reversible and irreversible changes in electrical conductivity and sub-bandgap absorption due to long term air and oxygen exposure. It was found that oxygen exposure caused an irreversible increase in σ_{Dark} and σ_{photo} and a decrease in the $\alpha(h\nu)$ spectrum in highly crystalline porous $\mu\text{c-Si:H}$, which could be due to oxygen permanently bonded to the surface of columns and grains. The effect of oxygen exposure for $\mu\text{c-Si:H}$ films with $I_C^{\text{RS}} < 0.70$ is much smaller and generally reversible. Finally, no significant changes were observed in the low crystalline and amorphous silicon films. Overall the changes in the observed parameters of thick $\mu\text{c-Si:H}$ films are rather small compared with earlier results on thinner films, which could mean that the effect of oxygen takes place only on the top surface of the films and the films get more compact with thickness.

Acknowledgement

We acknowledge financial support from TÜBİTAK of Turkey (project No. 108T218) and the BMBF of Germany (project No. TUR 08/003).

References

1. J. Meier, R. Flückiger, H. Keppner, and A. Shah. Appl. Phys. Lett. **65**, 860 (1994). doi:10.1063/1.112183.
2. O. Vetterl, R. Carius, L. Houben, C. Sholten, L. Luysberg, A. Lambertz, F. Finger, and H. Wagner. Mat. Res. Soc. Symp. Proc., **609**, A15.2 (2000).
3. D.L. Staebler and C.R. Wronski. Appl. Phys. Lett. **31**(4), 292 (1977). doi:10.1063/1.89674.
4. S. Veprek, Z. Iqbal, R.O. Kühne, P. Capezzuto, F.-A. Sarrot, and J.K. Gimzewski. J. Phys. C: Sol. State Phys. **16**, 6241 (1983). doi:10.1088/0022-3719/16/32/015.
5. F. Finger, R. Carius, T. Dylla, S. Klein, S. Okur, and M. Gunes. IEE Proc.-Circ. Dev. Sys. **150**, 300 (2003). doi:10.1049/ip-cds:20030636.
6. T. Dylla, F. Finger, and R. Carius. Mat. Res. Soc. Proc. **762**, A.2.5.1 (2003).
7. V. Smirnov, S. Reynolds, C. Main, F. Finger, and R. Carius. J. Non-Cryst. Solids, **338–340**, 421 (2004). doi:10.1016/j.jnoncrysol.2004.03.010.
8. V. Smirnov, S. Reynolds, F. Finger, R. Carius, and C. Main. J. Non-Cryst. Solids, **352**, 1075 (2006). doi:10.1016/j.jnoncrysol.2005.12.014.
9. R. Brüggemann and N. Souffi. J. Non-Cryst. Solids, **352**, 1079 (2006). doi:10.1016/j.jnoncrysol.2005.11.089.
10. G. Yilmaz, E. Turan, M. Günes, V. Smirnov, F. Finger, and R. Brüggemann. Physica Status Solidi C, **7**, 700 (2010). doi:10.1002/pssc.200982885.
11. M. Günes and C.R. Wronski. J. Appl. Phys. **81**(8), 3526 (1997). doi:10.1063/1.365000.
12. O. Goktas, N. Isik, S. Okur, M. Gunes, R. Carius, J. Klomfass, and F. Finger. Thin Solid Films, **501**, 121 (2006). doi:10.1016/j.tsf.2005.07.137.
13. M. Günes, H. Cansever, G. Yilmaz, V. Smirnov, F. Finger, and R. Brüggemann. J. Non-Cryst. Solids, **358**, 2074 (2012). doi:10.1016/j.jnoncrysol.2012.01.063.
14. M. Günes, H. Cansever, G. Yilmaz, H.M. Sagban, V. Smirnov, F. Finger, and R. Brüggemann. ICANS25 Proceedings. Manuscript in preparation. **92**, xxxx (2014).
15. D. Ritter and K. Weiser. Opt. Commun. **57**, 336 (1986). doi:10.1016/0030-4018(86)90270-1.
16. H. Cansever, G. Yilmaz, H.M. Sagban, M. Günes, V. Smirnov, F. Finger, and R. Brüggemann, ICANS25 Proceedings. Manuscript in preparation. **92**, xxxx (2014).
17. K. Lips, P. Kanschat, and W. Fuhs. Sol. Energy Mater. Sol. Cells, **78**, 513 (2003). doi:10.1016/S0927-0248(02)00450-6.
18. H. Fritzsche. In Electronic properties of surfaces in a-Si:H. Semiconductors and Semimetals, Vol. 21, Part C. Academic Press, Inc. 1984.